

# CELLO LOCAL SOLAR CELL RESISTANCE MAPS: MODELING OF DATA AND CORRELATION TO SOLAR CELL EFFICIENCY

J. Carstensen, A. Schütt, and H. Föll

Institute for Materials Science, Faculty of Engineering, Christian-Albrechts-University of Kiel,  
Kaiserstr. 2, 24143 Kiel, Germany, email: jc@tf.uni-kiel.de, Phone: (+49) 431 880 6181, Fax: (+49) 431 880 6178

**ABSTRACT:** CELLO (solar CELI LOcal characterization) allows to measure quickly and reliably local photo current and photo voltage responses. In this paper we present a fully general model, which allows to determine for which types of solar cells local diode and serial resistance data can be "averaged", and how that must be done in order to calculate the resistance parameter of the global IV curve. It turns out averaging of resistances is allowed for nearly all solar cells where the standard equivalent circuit can be used. This has been confirmed on a large number of solar cells and will be demonstrated here for mono- and multicrystalline solar cells.

**Keywords:** Serial resistances, Diode resistances, Characterization, Solar Cell Efficiencies

## 1 MODELING OF RESISTANCES IN SOLAR CELLS

### 1.1 Introduction

The CELLO (solar CELI LOcal characterization) technique analyzes the current and voltage response of a globally illuminated solar cell to local illumination with an intensity modulated LASER beam [1 - 5]. It is well known that local photo currents add up to the full photo current of the solar cell, resp. that the average of local photo currents scales with the global short circuit current. For local photo voltages there exists no such simple relation to the global photo potential. In this paper we will show that for a large number of solar cell types correspondingly simple averaging rules hold for photo resistances, i.e. the ratio between photo voltage and short circuit photo current. The averages of these local photo resistances are directly related to the corresponding parameter of the standard equivalent circuit, i.e. the (parallel) diode resistance and the serial resistance.

1.2 Resistance model of a solar cell that allows for analytical treatment.

The resistance network of a typical solar cell containing serial resistances represented by the metal grid and the emitter sheet resistance on top of the pn-junction and the junction resistance (represented by a strongly voltage dependent diode resistance) will be modeled by a circular "solar cell" (cf. Fig. 1 a) with a homogeneous emitter layer with sheet resistance  $\rho$  on top of a bulk layer. The pn-junction is characterized by a specific conductivity  $dj_{diode}/dU := K$ . We only will take into account this linear constant  $K$  since we are interested in the linear response of such a device, e.g. the (small) change  $dI_0$  of the current entering the circular solar cell when changing the externally applied voltage by  $dU_0$ . As will become clear from the final results the circular shape is not important; it just allows for simple analytical solutions. The full solar cell will be described as a parallel arrangement of several of these circular structures, connected by ohmic resistors.

The radial voltage distribution as a function of externally, i.e. from the periphery, applied current can be described by modified Bessel functions  $I_0$  and  $I_1$  as

$$dU(r) = \frac{dI_0 \rho}{2\pi \sqrt{\rho K} r_{\max}} \frac{I_0(\sqrt{\rho K} r)}{I_1(\sqrt{\rho K} r_{\max})}. \quad (1)$$

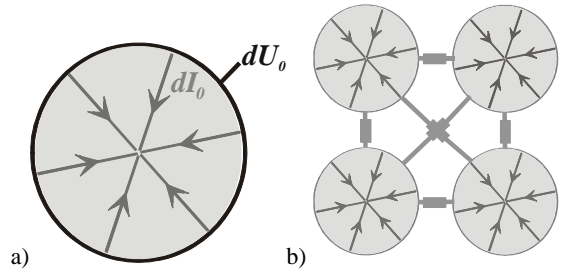


**Fig. 1:** Simple geometries for modeling resistance networks of solar cells.

Introducing a new variable for the relative area  $x := \pi r^2 / A$  ( $A$ : full area of circular solar cell), Eq. (1) can be rewritten as

$$R(x) := \frac{dU(x)}{dI_0} = \frac{\rho}{2\pi \sqrt{\rho K}} \frac{I_0\left(\sqrt{\frac{\rho K A x}{\pi}}\right)}{I_1\left(\sqrt{\frac{\rho K A}{\pi}}\right)} \quad (2)$$

Note that  $R(1) := R_{SC}$  represents the inverse slope of the global circular solar cell and thus is just the solar cell resistance for a certain externally applied voltage  $U$  and that due to charge conservation the diode resistance is

$$\frac{1}{R_D} := \frac{dI_{Diode}}{dU_0} = \frac{dj}{dU_0} = KA. \quad (3)$$

For  $\frac{\rho}{\pi R_D} = \frac{\rho K A}{\pi} < 1$  the Bessel function  $I_0$  can be written as

$$I_0\left(\sqrt{\frac{\rho K A x}{\pi}}\right) \approx 1 + \frac{1}{4} \frac{\rho K A x}{\pi} + \frac{1}{60} \left(\frac{\rho K A x}{\pi}\right)^2 \approx 1 + \frac{1}{4} \frac{\rho K A x}{\pi}.$$

We now can simplify Eq. (2) to

$$R(x) = \frac{1}{KA} \frac{1 + \frac{1}{4} \frac{\rho K A x}{\pi}}{1 + \frac{1}{8} \frac{\rho K A}{\pi}} = R_D \frac{1 + \frac{1}{4} \frac{\rho x}{\pi R_D}}{1 + \frac{1}{8} \frac{\rho}{\pi R_D}}. \quad (4)$$

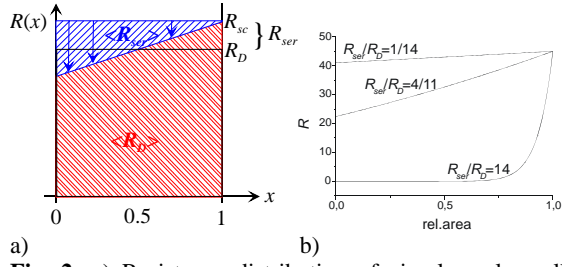


**Fig. 2:** a) Resistance distribution of circular solar cell according to Eq. (4). b) Resistance distribution of Eq. (2) for several fractions of  $R_{ser} / R_D$ .

Fig. 2a illustrates Eq. (4) and its consequences. The area below the curve  $R(x)$  represents the integral current flowing across the pn-junction. Due to charge conservation this equals  $dI_0$ . According to the definition of  $R(x)$  and reflecting Eq. (3) the average of this curve is  $R_D$  as indicated by the horizontal line. Ignoring the shunt resistance, the global resistance of a solar cell  $R_{SC} = R(1)$  is just the sum of the diode resistance  $R_D$  and the serial resistance  $R_{ser}$  which allows to calculate

$$R_{ser} := R_{sc} - R_D = R(1) - R(0.5) \quad (5)$$

Using Eq. (4) one finally obtains

$$\frac{1}{R_{ser}} = \frac{1}{\frac{1}{8\pi}\rho} + \frac{1}{R_D} := \frac{1}{R_{ser,\infty}} + \frac{1}{R_D} \quad (6)$$

The effective sheet resistance  $\rho$  is constant, i.e. it does not depend on the externally applied voltage  $U$ . This is not true for  $R_D$ , which exponentially decreases in forward direction. To apply the standard equivalent circuit for the description of the global IV curve of a solar cell it is therefore necessary that  $R_D$  is much larger than  $R_{ser}$  for all measured points along the IV curve. It is important to realize that this condition may not be fulfilled near open circuit conditions. Interpreting Eq. (6), the externally measured serial resistance is a parallel arrangement of the sheet resistance and the diode resistance. As long as the pn-junction is blocking, the serial resistance is only defined by the sheet resistance and stays constant. If a reasonable amount of current leaves the emitter across the pn-junction even at low voltages, the current flowing laterally through the emitter is reduced and the effective serial resistance becomes smaller.

Rewriting the condition for which Eq. (4) holds we get

$$\frac{\rho}{\pi R_D} = \frac{8R_{ser}}{R_D} < 1; \quad (7)$$

so we can state that as long as a linear lateral voltage distribution is found, the standard equivalent circuit adequately describes the IV curve of a large area solar cell. The lateral voltage, or the resistance distribution, respectively, has a second, very important consequence which is illustrated in the upper part of Fig. 2a). Lateral ohmic losses are indicated by the reduction of  $R(x)$  for  $x < 1$ . Averaging this local serial resistance losses across the solar cell, i.e. averaging the area of the upper triangle, we get the serial resistance  $R_{ser}$  according to the definition of the standard equivalent circuit. This is not true for all types of solar cells as can be easily seen from Fig. 2b) which shows the resistance distribution of Eq. (2) for

several fractions of  $R_{ser}$  and  $R_D$ . If  $R_{ser} / R_D > 1$  obviously no averaging rule for local serial resistances holds.

We will not go into the details for the mathematics and interpretation of the more general model for describing real solar cells as in Fig. 1b). It is sufficient to mention here that all results with respect to averaging serial resistances, applicability of the standard equivalent circuit, and finding a linear lateral voltage distribution still hold if adding a real ohmic resistance in series and putting several of such (identical) elements in parallel. An ohmic serial resistor just shifts the average and putting  $N$  elements in parallel just reduces the slope and the offset of the lateral resistance distribution by the factor  $N$ . Even if the condition (7) is not fulfilled the serial resistance for the model in Fig. 1b) may be well described by

$$R_{ser} = R_{ser,busbars} + \frac{1}{\frac{1}{R_{ser,\infty}} + \frac{1}{R_D}} \quad (8)$$

## 2 COMPARISON WITH EXPERIMENTAL RESULTS

### 2.1 Results from a homogeneous mono Si solar cell

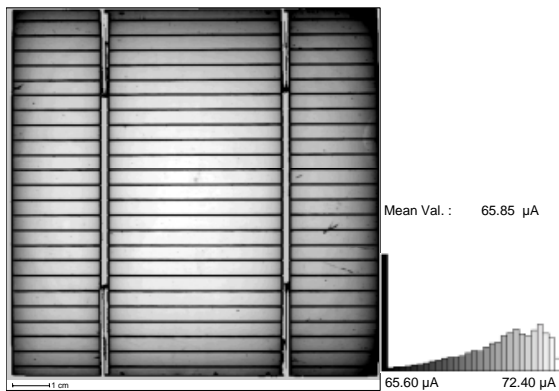
Since the standard equivalent circuit has been successfully used to describe nearly all solar cells, one may expect that the results of this paper with respect to the linear lateral resistance distribution and averaging of serial resistances should work on all these solar cells as well. For verifying this, the first question which has to be solved is how one can generate resistance maps, resp. resistance distributions as described in Eq. (4) or illustrated in Fig. 1a) from CELLO measurements. In principle this is very simple: Just divide local CELLO photo voltage data by the local short circuit photo current maps as shown in Fig. 3 a)-c). We will omit here some of the tricky details for interpreting the CELLO results, which, e.g., are related to the fact that we use 4 reference electrodes for measuring photo voltages. The distribution function can now be easily calculated from the histogram  $H(R)$  of Fig. 3c). Integrating

$$N(R) := \int_0^R H(R) dR \quad (9a)$$

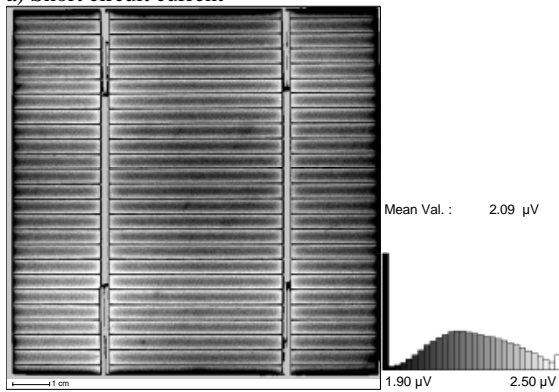
and dividing

$$x(R) := \frac{N(R)}{N(\infty)} \quad (9b)$$

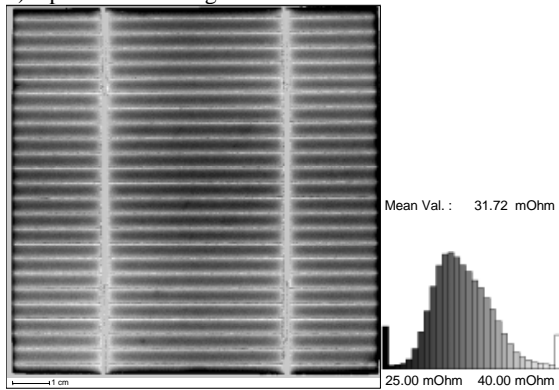
one gets  $R(x)$  just by inverting Eq. (9b). For the resistance map in Fig. 3c) this procedure gives the resistance distribution shown in Fig. 3d). As expected from the theory discussed above, we find a straight line for a large fraction of the solar cell area. Combining the slope of this curve and the slope of the IV curve at open circuit as indicated by the tangent in Fig. 3e) allows to calculate the map of the local serial resistances (cf. Fig. 3f). We skip the details here because this would need a more detailed discussion of the model in Fig. 1b). Of course the theory is not limited to open circuit condition but can (even more generally) be applied to e.g. the working point of the solar cell. The results for the resistance map and the resistance distribution are shown in Figs. 3g) and 3h). Subtracting, e.g., in a second step the serial resistance one can calculate the map of the pure diode resistance at the working point of the solar cell. In the example shown in Fig. 3i) areas of decreased (bad) local diode resistances are visible around the edge of the solar cell.



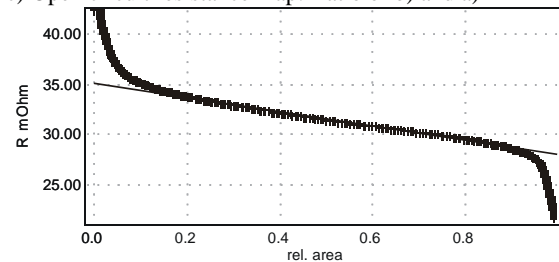
a) Short circuit current



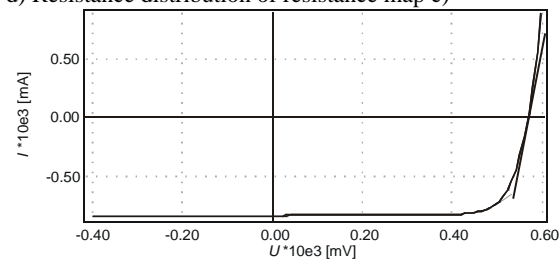
b) Open circuit voltage



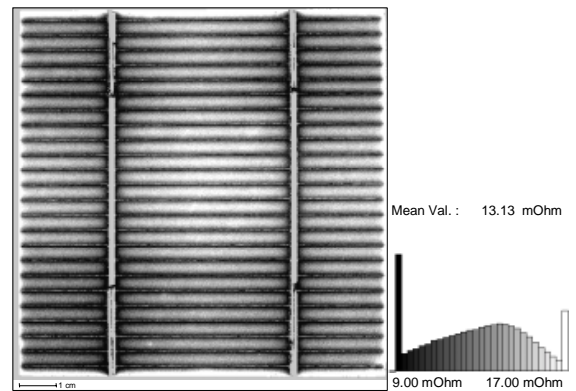
c) Open circuit resistance map: Ratio of b) and a)



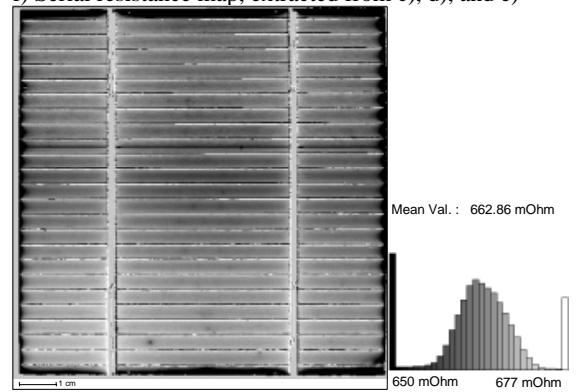
d) Resistance distribution of resistance map c)



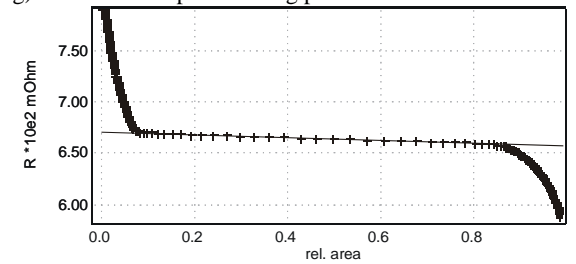
e) IV curve of the solar cell



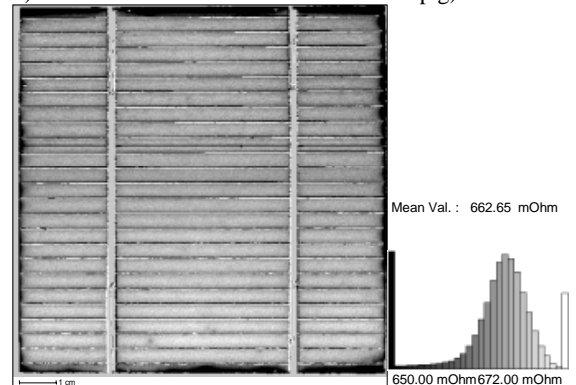
f) Serial resistance map, extracted from c), d), and e)



g) Resistance map at working point of solar cell

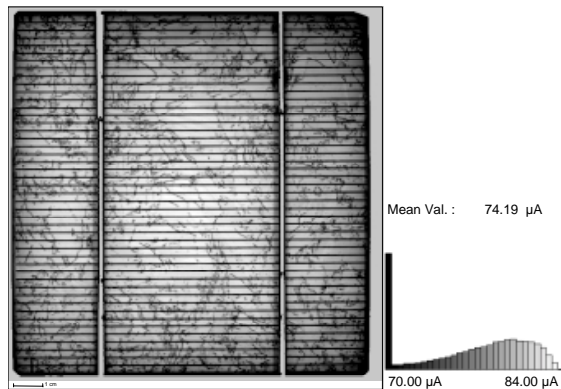


h) Resistance distribution of resistance map g)

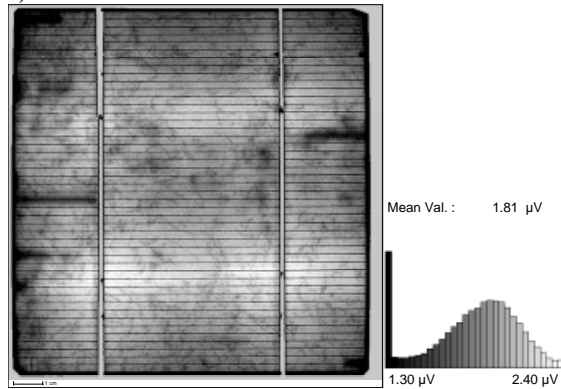


i) Diode resistance map at working point, calculated by "subtracting" the serial resistance map f) from map g).

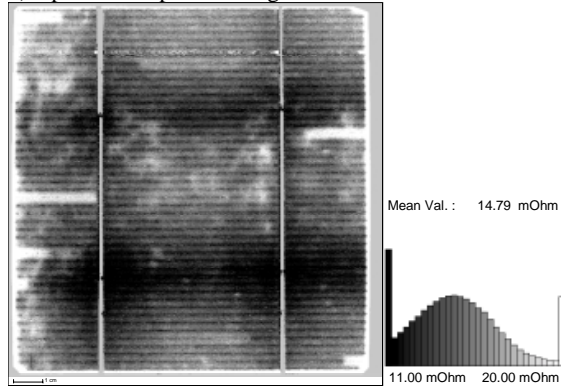
**Fig. 3:** CELLO photo current and photo voltage maps for a 10 cm x 10 cm mono Si solar cell. Combining these maps, extracting lateral distribution functions, and taking into account the corresponding slopes of the global IV curve allows to calculate local resistance maps as indicated in the figure captions.



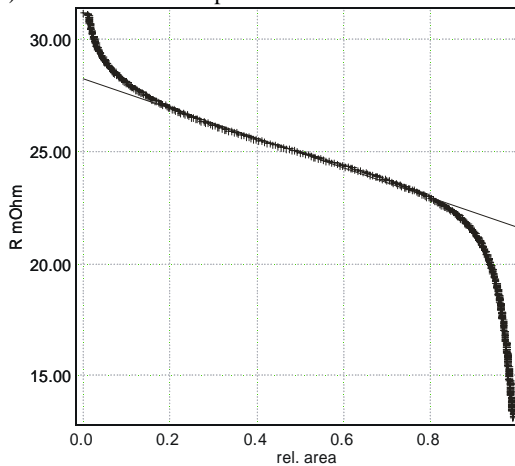
a) Short circuit current



b) Open circuit photo voltage



c) Serial resistance map



d) Resistance distribution of ratio map b) / map a)

**Fig. 4:** CELLO results on mc-Si solar cell. Here as well a linear lateral resistance distribution is found.

## 2.2 Results on a typical multicrystalline Si solar cell

Due to the averaging procedure in Eq. (9) local inhomogeneities do neither spoil the procedure nor the model for calculating local resistances and resistance averages as illustrated for the mc-Si solar cell in Fig. 4. Again the resistance distribution shows a large linear regime. The slope of the straight fitting line allows to calculate local the serial resistance as shown in Fig. 4c). In this map clearly broken grid fingers are visible, for example. In addition, the upper left part of the solar cell shows a larger region with increased serial resistances, which most probably are related to contact problems between emitter and grid. The evaluation of a large number of such solar cells shows that the model described in this paper works as long as resistance problems are not directly correlated to other defect types like e.g. strongly recombination active defects. In the example shown in Fig. 4 the model works, because broken grid fingers are found in regions with and without grain boundaries, which is the typical case. For most solar cells lateral serial and diode resistances could be correctly analyzed. In addition, using the serial resistance model in Eq. (8) and fixing the non ideality factor for the second diode  $n_2 = 2$ , gave almost always better fitting results than the standard model, because the condition (7) is not fulfilled for most solar cells for open circuit.

## 3 SUMMARY AND CONCLUSIONS

A new model-based analysis backed-up by experiments demonstrates that for a large number of solar cells averaging rules exist for the local serial and diode resistances that allow to calculate the corresponding global resistances. This allows a fully quantitative analysis of the influence of certain defect types on the solar cell efficiency by analyzing CELLO photo current and photo voltage maps. Further consequences of this model, especially on the general impact of the grid design on loss mechanisms, will be presented elsewhere.

## 4 REFERENCES

- [1] J. Carstensen, G. Popkirov, J. Bahr, and H. Föll, in *Proceedings of the 16th European Photovoltaic Solar Energy Conference*, VD3.35, Glasgow (2000).
- [2] J. Carstensen, G. Popkirov, J. Bahr, and H. Föll, *Solar Energy Materials & Solar Cells* **76**, 599 (2003).
- [3] J. Carstensen, S. Mathijssen, G. Popkirov, and H. Föll, in *Proceedings of the 20th European Photovoltaic Solar Energy Conference*, 1AV.2.40, Barcelona (2005).
- [4] J. Carstensen, A. Schütt, G. Popkirov, and H. Föll, in *Proceedings of the 21th European Photovoltaic Solar Energy Conference*, 2AO.3.4, Dresden (2006).
- [5] A. Schütt, J. Carstensen, and H. Föll, in *Proceedings of the 21th European Photovoltaic Solar Energy Conference*, 1BV.2.36, Dresden (2006).